Polymer 55 (2014) 525–534

Contents lists available at ScienceDirect

Polymer

journal homepage: www.elsevier.com/locate/polymer

pH- and temperature-responsive amphiphilic diblock copolymers of 4-vinylpyridine and oligoethyleneglycol methacrylate synthesized by RAFT polymerization

Murat Topuzogullari [a], Volga Bulmus [b], Eray Dalgakiran [a], Sevil Dincer [c,*]

[a] Yildiz Technical University, Department of Bioengineering, Davutpasa, Istanbul, Turkey
[b] İzmir Institute of Technology, Department of Chemical Engineering, Urla, İzmir, Turkey
[c] Abdullah Gul University, Materials Science and Nanotechnology Engineering, Kayseri, Turkey

ARTICLE INFO

Article history:
Received 30 September 2013
Received in revised form
9 December 2013
Accepted 17 December 2013
Available online 28 December 2013

Keywords:
Amphiphilic block copolymers
RAFT polymerization
Stimuli-responsive

ABSTRACT

Diblock copolymers of 4-vinylpyridine (4VP) and oligoethyleneglycol methyl ether methacrylate (OEGMA) were synthesized for the first time using RAFT polymerization technique as potential drug delivery systems. Effects of the number of ethylene glycol units in OEGMA, chain length of hydrophobic P4VP block, pH, concentration and temperature on the solution behavior of the copolymers were investigated comprehensively. Copolymer chains formed micelles at pH values higher than 5 whereas unimeric polymers were observed to exist below pH 5, owing to the repulsion between positively charged P4VP blocks. The size of the micelles was dependent on the relative length of blocks, P4VP and POEGMA. Thermo-responsive properties of copolymers were investigated depending on the pH and length of P4VP block. The increase in the length of P4VP block decreased the LCST substantially at pH 7. At pH 3, LCST of copolymers shifted to higher temperatures due to the increased interaction of co-polymers with water through positively charged P4VP block.

1. Introduction

Amphiphilic block copolymers (ABC) have become an important class of building elements for drug carrier systems owing to their ability to form micelles and nanoaggregates, high structural stability, loading capacity and water solubility [1]. ABCs form micelles in aqueous solutions through association of unimeric copolymer chains, which is an entropy and enthalpy driven process [2]. Hydrophobic segments of the copolymers constitute the core of the micelle in which hydrophobic drugs can be loaded. The shell of the micelle is comprised of the hydrophilic blocks of the copolymers, making the particle water-dispersible. Size, chain lengths and molar ratio of blocks, molecular weight and shell-forming block chemistry are some of the properties that affect the biological activity of micelles of ABCs [1,3,4].

Efficacy and capabilities of ABC micelles in physiological conditions can be improved by adding stimuli-responsive elements to the structure [5]. For example, micelles of pH-responsive ABCs can release their cargo molecules at a given pH specific to a tissue, such as intestine or stomach [6], in tumor tissue [7]. Micelles of temperature-responsive polymers can display improved tissue-targeting capability using local hyperthermia techniques [8].

In order to better understand the structure–function relationship and to obtain reproducible results in biological studies, it is vital to use polymers with a well-defined structure and uniform character [9]. Controlled radical polymerization techniques allow us to synthesize near monodisperse, well-defined polymers in a precise way. RAFT (reversible addition-fragmentation chain transfer) polymerization, one of the mostly used controlled radical polymerization techniques, has been increasingly used for producing polymers to be used in biological applications [10]. The technique can be applied to almost all vinyl monomers by using a proper chain transfer agent [11,12]. RAFT polymerization is a versatile technique for the synthesis of end-functionalized polymers and polymers with diverse structures such as block, graft, star and gradient polymers [10,13].

Poly(2-vinylpyridine) (P2VP), poly(4-vinylpyridine) (P4VP) and their copolymers with various monomers have been used in several biomedical applications, such as drug release systems [14,15], gene therapy studies [16] and antimicrobial polymeric systems [17,18]. One of the main advantages of poly(vinylpyridine)s in bio-applications is their pH-responsive nature arose from the

* Corresponding author.
E-mail addresses: sevild77@gmail.com, sevil.dincer@agu.edu.tr (S. Dincer).

0032-3861/$ – see front matter © 2013 Elsevier Ltd. All rights reserved.
http://dx.doi.org/10.1016/j.polymer.2013.12.040

alteration of their solubility in aqueous solutions upon pH change. At acidic pH values, tertiary amine in pyridine ring of poly(-vinylpyridine) is protonated and positively charged, making the polymer chains hydrophilic while poly(vinylpyridine) chains become relatively hydrophobic and insoluble at neutral and basic pH values because of the deprotonation of pyridine amine. Poly(-vinylpyridine)s can be made soluble and positively charged at all pH values by partial quaternization of tertiary amine in pyridine ring. By changing the structure of quaternizing agent, hydrophobicity and solution behavior of poly(vinylpyridine)s can easily be adjusted [16].

Poly(oligoethylene glycol methyl ether methacrylate) (POEGMA) is a non-immunogenic, non-toxic, uncharged and water-soluble biocompatible polymer like poly(ethylene glycol) (PEG) [19,20]. RAFT technique can easily be applied to polymerize OEGMA monomers [21]. Polymers having an LCST (lower critical solution temperature) can be synthesized by copolymerizing DEGMA (diethylene glycol methyl ether methacrylate) and OEGMA monomers. The LCST value of ethylene glycol methacrylate copolymers can be fine-tuned by changing the initial comonomer ratio and the number of ethylene glycol units in OEGMA monomer [22].

In this study, we synthesized di-block copolymers of P4VP and POEGMA as a potential drug release system using RAFT polymerization technique. All copolymers synthesized were near monodisperse and had α-carboxylic acid functionalized POEGMA block suitable for conjugation of a targeting or labeling molecule. Although copolymers of 4VP or OEGMA with different monomers [15,23–25] and with each other [17,18] in diverse structures have been examined previously, block copolymers of these monomers have been investigated for the first time. To obtain stimuli-responsive and tunable structures as potential controlled drug release systems, the effects of side chain length of POEGMA block, length of P4VP block, pH, temperature and concentration on solution behavior of POEGMA-*b*-P4VP copolymers were thoroughly investigated. These dual-responsive block copolymers have potential to be used as carriers in drug release by the local change in pH or temperature.

2. Experimental

2.1. Materials

$OEGMA_{475}$ (M_n = 475 g/mol), $OEGMA_{950}$ (M_n = 950 g/mol), diethylene glycol methyl ether methacrylate (DEGMA) and 4VP were purchased from Aldrich. Azobisisobutyronitrile (AIBN) was purchased from Aldrich and recrystallized from methanol before using. 4-Cyano-4-(thiobenzoylthio)pentanoic acid (under license from CSIRO) was obtained from Strem Chemicals, Inc. Pyrene (Aldrich) was recrystallized from ethanol. Ultra-pure water was obtained from Millipore MilliQ Gradient system. All other chemicals used were analytical grade.

2.2. Synthesis of POEGMA polymers (MacroCTAs)

Two homopolymers ($POEGMA_{475}$ and $POEGMA_{950}$) and a copolymer (P(DEGMA-*co*-$OEGMA_{475}$)) were first synthesized as macroCTAs. Molar ratio of comonomers in the feed was $n_{OEGMA475}/n_{DEGMA}$ = 8/92 in P(DEGMA-*co*-$OEGMA_{475}$) copolymer synthesis.

RAFT polymerization of $OEGMA_{475}$ is as follows: A $[M]_0/[CTA]_0/[I]_0$ ratio of 75/1/0.2 were used for RAFT polymerization of 0.5 M $OEGMA_{475}$. AIBN was used as an initiator and 4-cyano-4-(thiobenzoylthio)pentanoic acid was used as a chain transfer agent (CTA). 2.85 g $OEGMA_{475}$ (6 mmol), 22.35 mg CTA (0.08 mmol) and 3.43 mg AIBN (0.021 mmol) were dissolved in DMF (9.1 mL). Solution was purged with N_2 for 30 min and sealed with a septum. Solution was heated to 70 °C in an oil bath. An aliquot of 1 mL was withdrawn from the reaction mixture every hour using a syringe while purging with N_2. Samples were precipitated in cold diethyl ether. Precipitates were dissolved in dichloromethane and precipitated in ether again. Samples were dried under vacuum overnight and final products that were pink-colored polymers were obtained. Monomer conversion was calculated gravimetrically. All samples were analyzed with NMR spectroscopy and GPC.

Same procedure was followed for $POEGMA_{950}$ and P(DEGMA-*co*-$OEGMA_{475}$) synthesis using different $[M]_0/[CTA]_0/[I]_0$ ratios and monomer concentrations to obtain polymers with identical molecular weights. $POEGMA_{950}$ was synthesized by polymerization of 0.25 M $OEGMA_{950}$ using a $[M]_0/[CTA]_0/[I]_0$ ratio of 75/1/0.2. A $[M]_0/[CTA]_0/[I]_0$ ratio of 150/1/0.2 was used for copolymerization of 0.92 M DEGMA and 0.08 M $OEGMA_{475}$ to obtain P(DEGMA-*co*-$OEGMA_{475}$) copolymer.

2.3. Synthesis of POEGMA-b-P4VP block copolymers

$POEGMA_{475}$, $POEGMA_{950}$ and P(DEGMA-*co*-$OEGMA_{475}$) polymers were used as macroCTAs for preparation of POEGMA-*b*-P4VP copolymers.

Polymerization of 4VP from $POEGMA_{475}$ macroCTA is as follows: A $[M]_0/[CTA]_0/[I]_0$ ratio of 200/1/0.5 and a monomer concentration of 1.5 M were used for the synthesis of $POEGMA_{475}$-*b*-P4VP. $POEGMA_{475}$ with a M_n of 17,200 g/mol and PDI of 1.14 was used as a macroCTA. 0.32 g 4VP (3 mmol), 0.26 g macroCTA (0.015 mmol) and 1.23 mg AIBN (0.008 mmol) were dissolved in 1.65 mL DMF. Solution was purged with N_2 for 30 min and sealed with septum. Solution was heated to 70 °C in oil bath. Aliquots of 1 mL were withdrawn from the reaction mixture after 3 and 6 h using a syringe while purging with N_2. Samples were precipitated in cold diethyl ether. Precipitates were dissolved in dichloromethane and precipitated in diethyl ether again. Samples were dried under vacuum overnight and final products were obtained as orange-brown colored polymers. Monomer conversion was calculated gravimetrically. All samples were analyzed using NMR spectroscopy and GPC.

Block copolymers of $POEGMA_{950}$ and P(DEGMA-*co*-$OEGMA_{475}$) macroCTAs were synthesized using the same procedure with the same $[M]_0/[CTA]_0/[I]_0$ ratio and monomer concentration.

2.4. Characterizations

^1H NMR spectra of all polymers were acquired from Bruker Avance III 500 MHz NMR spectrometry. All homo- and copolymers were dissolved in $CDCl_3$ for NMR analyses.

GPC chromatograms were acquired using a Viscotek TDA302 GPC system with refractive index (RI) and light scattering at 90° (LS) detectors. Viscotek GPCmax auto-sampler was used for mobile phase flow and sample injections. HPLC grade THF was used as a mobile phase at a flow rate of 0.8 mL/min. Shimadzu Shim-Pack GPC804 GPC column was used for separations and all chromatograms were acquired at ambient temperature. Detectors were calibrated using a linear polystyrene standard (M_w = 99,000 g/mol, PDI = 1.05, dn/dc = 0.165) purchased from Viscotek. All samples were dissolved in THF and filtered through 0.2 μm pore-sized PTFE syringe filters. Injection volume was 100 μL.

Solution behavior of block copolymers was investigated with fluorescence spectrometry and light scattering techniques. Block copolymers were dissolved at various concentrations and pH values in 6×10^{-7} M pyrene containing 0.02 M phosphate buffers. In fluorescence spectrometry measurements, samples were excited between 300 and 360 nm and excitation spectra were acquired by measuring the emission at 390 nm. Slit aperture was 2 nm and

spectra were recorded at 0.5 nm/0.5 s rate. Intensity ratio of 338 nm–333 nm was calculated for each sample to understand the hydrophobicity of pyrene's microenvironment [26]. Zetasizer Nano ZS (Malvern) instrument was used for dynamic and electrophoretic light scattering measurements to obtain hydrodynamic diameters and zeta potentials of block copolymers. All samples were filtered through 0.2 μm pore-sized syringe filters before analyzes. Size and zeta potential measurements were acquired at 25 °C, with the exception of temperature-responsive copolymers which were analyzed at 15 °C to prevent agglomeration. Transmittance measurements of copolymer solutions were performed at 550 nm using Shimadzu UV-1700 UV-VIS spectrophotometer with CPS-240A temperature control unit.

Shimadzu SPM 9600 atomic force microscope in dynamic mode was used for the morphological examination of block copolymers. 5 μL of aqueous block copolymer solutions (1 mg/mL) were dropped to freshly cleaved mica surface and incubated for 5 min. Mica surface was rinsed with water and dried for 20 min.

3. Results and discussion

3.1. Synthesis of polymers

In this study, we aimed to synthesize POEGMA-*b*-P4VP amphiphilic diblock copolymers for the first time and investigate the effects of structural alterations on their solution behavior. We prepared 3 different sets of block copolymers using three different oligoethylene glycol methacrylate based macroRAFT agents having similar number average molecular weights (M_n) but varying number of ethylene glycol repeating units in their side chains (POEGMA$_{475}$, POEGMA$_{950}$ and P(DEGMA-*co*-OEGMA$_{475}$) having a M_n between 17,200 and 19,100 g/mol. Two POEGMA-*b*-P4VP copolymers with varied chain lengths of P4VP blocks were then synthesized using each POEGMA based macroRAFT agent (Scheme 1).

Fig. 1 gives kinetic plots of RAFT polymerization of OEGMA based monomers for the synthesis of macroRAFT agents. As seen in Fig. 1a, pseudo-first order kinetics was observed for polymerization of OEGMA$_{475}$ ($[M]_0/[CTA]_0/[I]_0 = 75/1/0.2$ and $[M]_0 = 0.5$ M) with a short retardation period. In Fig. 1b, molecular weight (M_n) and polydispersity index values of OEGMA$_{475}$ polymers are given depending on the monomer conversion. M_n of the OEGMA$_{475}$ homopolymers increased linearly with the increase in monomer conversion. Polydispersity indexes of homopolymers were below 1.2. The only homopolymer with a PDI above 1.2 was obtained in the first hour of polymerization (at very low conversion), as expected due to the retardation period. GPC-LS chromatograms of OEGMA$_{475}$ homopolymers are given in Fig. 1c. The retention volumes of homopolymers reduced with the increase in reaction time, indicating the formation of higher molecular weight polymers with increasing time. In addition, peak areas increase in accordance with increasing time. LS signals are directly related to concentration, dn/dc and molecular weight of polymers. Increase in peak areas in Fig. 1c indicates the molecular weight (M_n) increase, since the concentration and dn/dc of all samples in chromatograms are identical.

The results belonging to RAFT copolymerization of OEGMA$_{475}$ (8% mol) and DEGMA (92% mol) are given in Fig. 1d–f. A $[M]_0/[CTA]_0/[I]_0$ of 150/1/0.2 ratio ($[M]_0 = 1$ M) was used in polymerization to obtain P(DEGMA-*co*-OEGMA$_{475}$) having a molecular weight similar to that of POEGMA$_{475}$ macroRAFT agent. Copolymer composition is expected to be very close or identical to the monomer feed composition [22]. Fig. 1d shows the monomer conversion and pseudo-first order kinetics of polymerization.

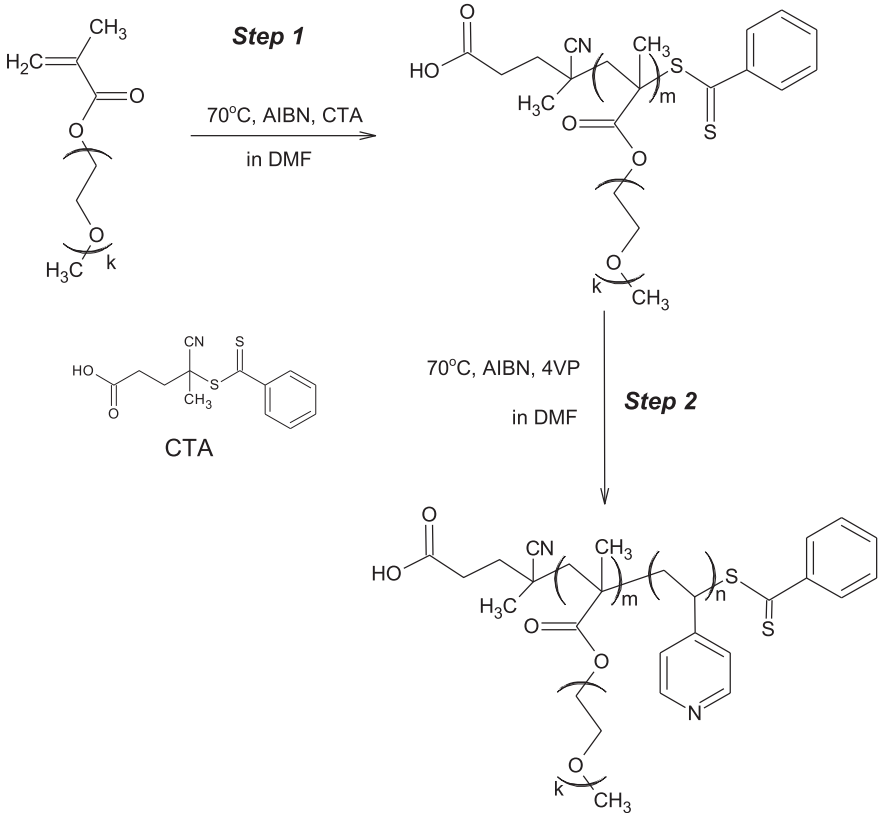

Scheme 1. Schematic representation of the synthesis of POEGMA-*b*-P4VP block copolymers via RAFT polymerization.

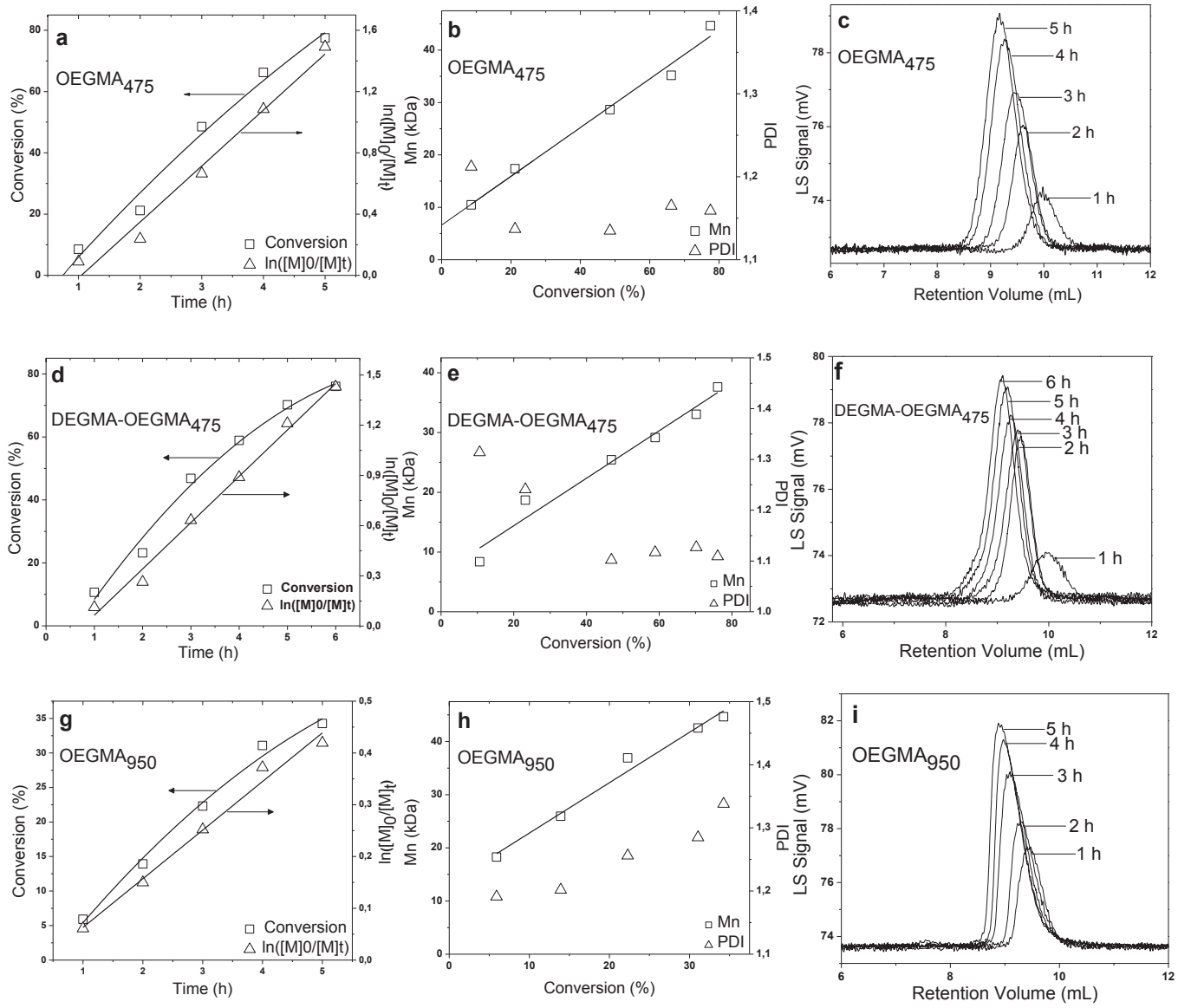

Fig. 1. Kinetics of RAFT polymerization of $OEGMA_{475}$ (a), DEGMA-$OEGMA_{475}$ (d) and $OEGMA_{950}$ (g). Relationship between molecular weight and polydispersity index with monomer conversion of $OEGMA_{475}$ (b), DEGMA-$OEGMA_{475}$ (e) and $OEGMA_{950}$ (h) polymerizations. Evolution of GPC chromatograms of $POEGMA_{475}$ (c), P(DEGMA-*co*-$OEGMA_{475}$) (f) and $POEGMA_{950}$ (i) at different times of RAFT polymerization acquired from LS detector (concentrations of all samples were identical in GPC analyses).

Retardation in initial stage of polymerization was also seen in this reaction. Molecular weight (M_n) linearly increased with monomer conversion. Polydispersity indexes of polymers were higher (1.31 and 1.24, respectively) in early stages of polymerization as expected and reduced with increasing monomer conversions. The shift of GPC peaks to smaller retention volumes and the increase in LS peak areas in GPC chromatograms (Fig. 1f) clearly showed the increase in molecular weight of P(DEGMA-*co*-$OEGMA_{475}$) with increasing reaction time. Polymers show unimodal distributions in chromatograms.

RAFT polymerization of $OEGMA_{950}$ was conducted using a $[M]_0/[CTA]_0/[I]_0$ ratio of 75/1/0.2 and a monomer concentration of 0.25 M (Fig. 1g–i). Monomer conversion was lower when compared with the conversions obtained with $POEGMA_{475}$ and P(DEGMA-*co*-$OEGMA_{475}$). This was attributed to the lower initiator concentration which possibly prevented high conversions in polymerization. Molecular weight of polymers linearly increased with monomer conversion. Polydispersity index values were smaller than 1.3 and increased with monomer conversion. In GPC chromatograms, retention volumes of polymers reduced with reaction time. High viscosity of polymers and adsorption to GPC column material may have caused the asymmetry in GPC peaks of $POEGMA_{950}$ polymers.

Relatively high molecular weights were observed at the initial stages of RAFT polymerization of OEGMAs, when all M_n vs. conversion graphs presented in Fig. 1 are considered together. This phenomenon was explained by Pietsch et al. as a hybrid behavior [27] that free radical and RAFT polymerizations proceed together during RAFT pre-equilibrium. Short inhibition time observed in the beginning of polymerizations is caused by the rate retardation effect in dithiobenzoate mediated polymerizations [28]. Fig. 2a shows a typical ^1H NMR spectrum of $POEGMA_{475}$ homopolymer in $CDCl_3$. Resonance signals at 7.81, 7.46 and 7.30 ppm show aromatic protons of the RAFT agent. Methyl protons of methyl ether groups found in ethylene glycol side chain ends are observed at 3.32 ppm. Protons of methylene groups linked to methacrylate group are at 4.01 ppm. Overall, the unimodal distributions of polymer signals in GPC

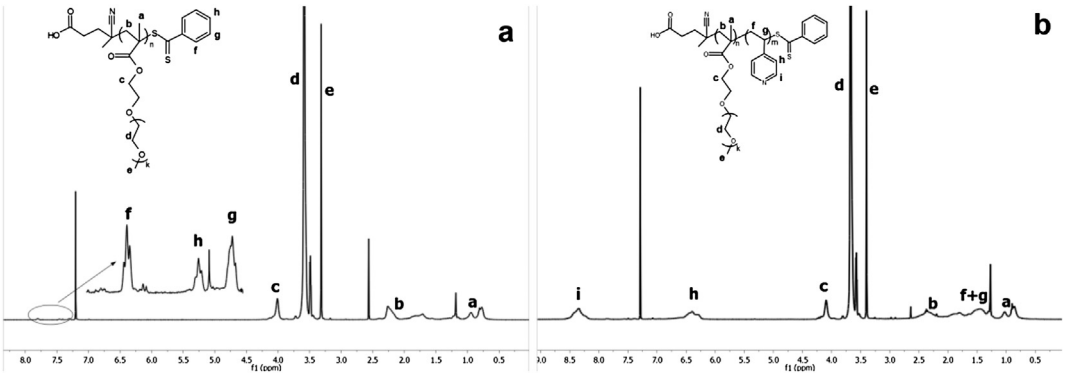

Fig. 2. ^{1}H NMR spectra of $POEGMA_{475}$ (a) and $POEGMA_{475}$-P4VP1 (b) in $CDCl_3$ at 18 °C. The peak at 7.25 ppm indicates $CHCl_3$ residue in solvent.

chromatograms, low polydispersity index values (<1.3), and linear evolution of molecular weights with conversions observed in RAFT polymerization of OEGMA monomers (Fig. 1) showed that well-defined and narrow disperse polymers were obtained in a controlled manner.

In the second step of synthesis, P4VP blocks were chain-extended from the POEGMA macroCTAs ($POEGMA_{475}$, $POEGMA_{950}$ and P(DEGMA-*co*-$OEGMA_{475}$)). Molecular weight and polydispersity index values of final block copolymer products are given in Table 1.

It is apparent that the molecular weight of macroRAFT agents increases with increasing reaction times, indicating the successful chain extension copolymerizations with 4VP. The P4VP block size also increases with reaction time. Polydispersity index values of all polymers are below 1.25. Low PDI values and increase in M_n with reaction time reveal the controlled manner of polymerizations of 4VP with POEGMA macroCTAs. As seen in Table 1, the copolymers having similar M_ns have P4VP blocks of identical chain lengths and varying POEGMA block structure (having varying length of oligoethyleneglycol grafts).

Fig. 3 shows GPC chromatograms of copolymers acquired from LS detector. Unimodal distributions and increase in peak areas with reaction time were observed in all chromatograms of copolymers, but tailings eluted after copolymer peaks indicate adsorption to column material. This may arise from lower solubility of P4VP block in THF. Minor decrease is observed in retention volumes of copolymers comparing to homopolymer chromatograms. This may be the result of conformational change, such as compaction, in polymer structure due to lower solubility of P4VP. In Fig. 2b, ^{1}H NMR spectrum of $POEGMA_{475}$-P4VP copolymer (M_n = 38200 g/mol, PDI = 1.09) is shown. In addition to $POEGMA_{475}$ peaks, three more signals in the spectrum indicate aromatic protons of pyridine rings (8.35 and 6.40 ppm) and protons of vinyl chain (1.48 ppm) of P4VP block.

Table 1
Molecular weight and polydispersity index values of block copolymers.

	Sample	Reaction time (*h*)	M_n (g/mol)	PDI
Set 1	$POEGMA_{475}$	0	17,200	1.14
	$POEGMA_{475}$-P4VP1	3	28,700	1.08
	$POEGMA_{475}$-P4VP2	6	38,200	1.09
Set 2	$POEGMA_{950}$	0	17,050	1.23
	$POEGMA_{950}$-P4VP1	3	30,100	1.12
	$POEGMA_{950}$-P4VP2	6	46,000	1.17
Set 3	P(DEGMA-*co*-$OEGMA_{475}$)	0	19,000	1.08
	P(DEGMA-*co*-$OEGMA_{475}$)-P4VP1	3	26,650	1.11
	P(DEGMA-*co*-$OEGMA_{475}$)-P4VP2	6	32,900	1.07

3.2. Critical micelle concentrations of copolymers

It is important to know the critical micelle concentration (*cmc*) of an ABC to be used as a building block for a drug carrier system. It is critical for micelles not to dissociate to unimers upon dilution with large volume of body fluids and not to release the therapeutic cargo before reaching the target tissue. One of the main advantages of ABCs is their very low *cmc* values in comparison with small surfactant molecules. Fluorescence spectrometry is a very sensitive technique and used for detecting *cmc* value of polymeric micelles by using a hydrophobic probe, such as pyrene. Band intensities in fluorescence spectrum of pyrene change according to the polarity of micro-environment in solution. *cmc* of ABC is detected by measuring the intensity ratio of pyrene in copolymer solution. Fig. 4 shows the change in intensity ratio of 6×10^{-7} M pyrene in copolymer solutions with varying concentrations at pH 7. Increase in I_{338}/I_{333} ratios reveals the hydrophobic environment around pyrene molecules entrapped in the core of ABC micelles [26]. P(DEGMA-*co*-$OEGMA_{475}$)-P4VP copolymers were observed to have the lowest *cmc* values, while $POEGMA_{950}$-P4VP copolymers had the highest (Table 2). These cmc values are much lower than low molecular weight surfactant micelles and convenient for drug release applications [29]. Above *cmc* values, copolymers with longer methacrylate chain but less ethylene glycol units have higher I_{338}/I_{333} values, which is attributed to higher pyrene loading of micelles.

With the increase in OEGMA length (i.e., $POEGMA_{950}$-P4VP), micelle formation occurs at higher concentrations because of increasing hydrophilicity comparing to the polymers having shorter OEGMA sequences (i.e., $POEGMA_{475}$-P4VP). On the other hand, hydrophobic methacrylate groups caused a decrease in *cmc* value as seen in Fig. 4c. Besides, the effect of POEGMA block on micelle formation seems to be more dominant than the effect of P4VP block, since the increase in P4VP chain length had a minor effect on *cmc* value.

In Fig. 4, open circles (○) belong to copolymers with longer P4VP chain and open squares (□) belong to copolymers with shorter P4VP chain. Above *cmc*, copolymers in each set behaved distinctly. In each set, copolymers with longer P4VP chains upto a certain concentration have higher I_{338}/I_{333} values. Above a certain concentration, I_{338}/I_{333} values of copolymers with longer P4VP blocks stayed constant or increased less than those of copolymers with shorter P4VP blocks. In contrast, fluorescence intensity ratios of copolymers with shorter P4VP blocks increased at all concentrations above *cmc*. The higher I_{338}/I_{333} values of copolymers with longer P4VP can be attributed to the stronger hydrophobic interactions between longer P4VP blocks that may lead to micelles with smaller sizes and aggregation number. This results in less

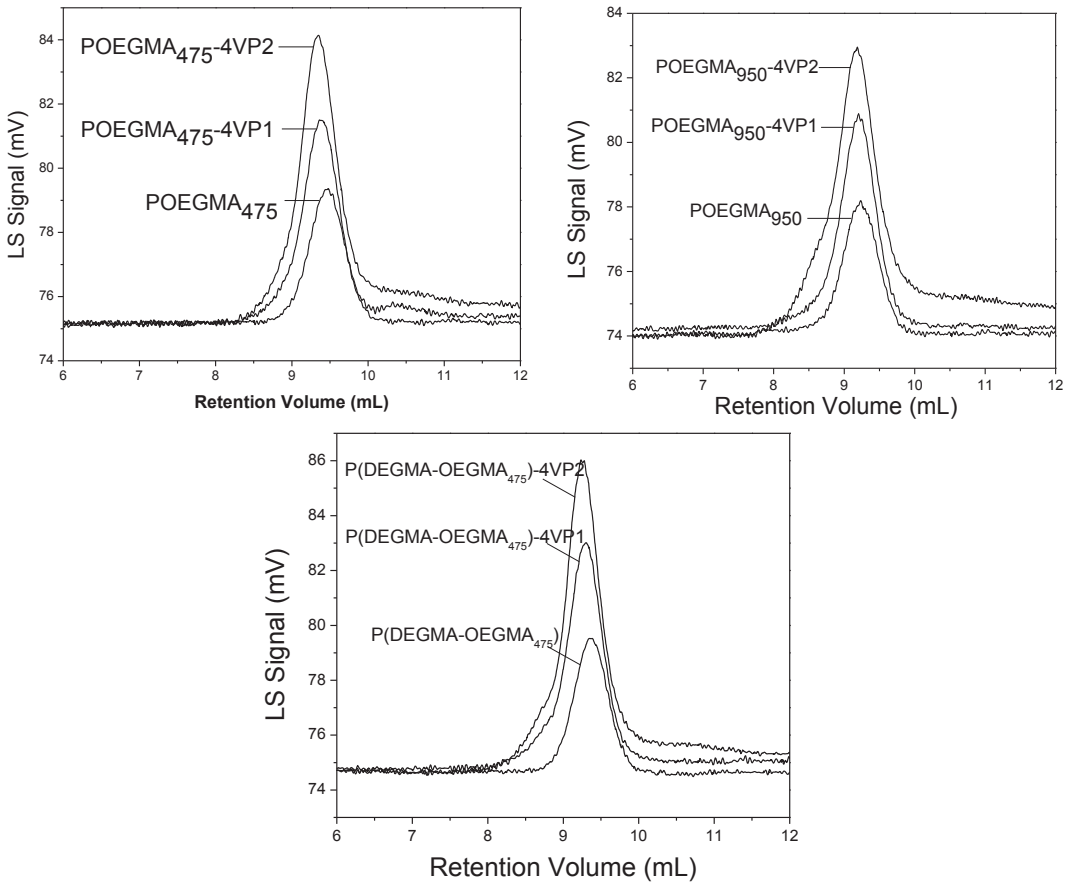

Fig. 3. Evolution of GPC chromatograms of $POEGMA_{475}$, P(DEGMA-*co*-$OEGMA_{475}$), $POEGMA_{950}$ and their copolymers with 4VP at different times of RAFT polymerization acquired from LS detector (concentrations of all samples were identical in GPC analyses).

pyrene molecules entering into the more hydrophobic core of copolymers with longer P4VP blocks. In contrary to this, micelles of copolymers with shorter P4VP blocks had a larger structure as a result of higher aggregation number and weaker hydrophobic interaction, and more pyrene molecules could be trapped in the cores of these copolymers' micelles.

3.3. *Effect of pH on solution behavior of copolymers*

P4VP block in copolymers is expected to be neutral and hydrophobic at basic or neutral pH but becomes water-soluble and positively charged at acidic pH values. Fig. 5 shows fluorescence intensity ratio (I_{338}/I_{333}) of 6×10^{-7} M pyrene in 1 mg/mL copolymer solutions as a function of pH. I_{338}/I_{333} ratios of copolymers were constant at pH values from 2 to 5 and only a slight decrease was observed in $POEGMA_{475}$-P4VP copolymers. It is apparent that values of I_{338}/I_{333} varied for copolymers with different POEGMA blocks between pH 2 and 5. I_{338}/I_{333} values of P(DEGMA-*co*-$OEGMA_{475}$)-P4VP copolymers between pH 2 and 5 were higher than those of other copolymers. The methacrylate chain length is the longest and the number of ethylene glycol units is the least in these copolymers. The opposite situation was true for $POEGMA_{950}$-P4VP copolymers. Structure of POEGMA block directly affects the number of pyrene molecules trapped in copolymer.

I_{338}/I_{333} ratios tend to increase at pH values higher than 5 for all copolymers. Copolymer unimers are expected to associate to form micelles above pH 5 with the driving force of hydrophobic interactions between deprotonated P4VP blocks. Hence, more pyrene molecules could be confined in the P4VP core of the micelles. As seen in Fig. 5, a slight increase in I_{338}/I_{333} ratio of P(DEGMA-*co*-$OEGMA_{475}$)-P4VP copolymers was observed when compared with the ratio of other copolymers. We can say that most pyrene molecules are trapped by hydrophobic methacrylate chain in P(DEGMA-*co*-$OEGMA_{475}$) block of the copolymer and micelle formation has a minor effect on loading capacity of copolymers. In other copolymers ($POEGMA_{475}$-P4VP and $POEGMA_{950}$-P4VP), I_{338}/I_{333} ratio increased markedly, which indicates the entrapment of pyrene molecules into the P4VP core of the micelle. Micelle formation has major effect on pyrene loading capacity of $POEGMA_{475}$-P4VP and $POEGMA_{950}$-P4VP copolymers due to the more hydrophilic nature of POEGMA blocks. As a general assessment in terms of drug delivery, drug molecules entrapped in these micelles may be released by the decrease in pH.

Fig. 6 shows hydrodynamic sizes and zeta potentials of copolymers as a function of solution pH. The hydrodynamic diameters were obtained from size distributions by volume. 6×10^{-7} M pyrene was added to all copolymer solutions for comparison with fluorescence results. Below pH 5, diameter of copolymers varies between 5 and 7 nm. In each set of copolymers, average diameters of polymers increase with increasing P4VP chain length. Diameters of copolymers below pH 5 increase from 6.1 to 7.0 nm for $POEGMA_{475}$-P4VP, from 6.5 to 6.8 nm for $POEGMA_{950}$-P4VP and from 5.1 to 5.9 nm for P(DEGMA-*co*-$OEGMA_{475}$)-P4VP copolymers when P4VP block size was increased. The increase in the hydrodynamic diameters below pH 5 is not at the same extent with the increase in the degree of polymerization in copolymers with longer P4VP blocks. This can be attributed to the fact that copolymer chains adopt a random coil to globular conformation, instead of

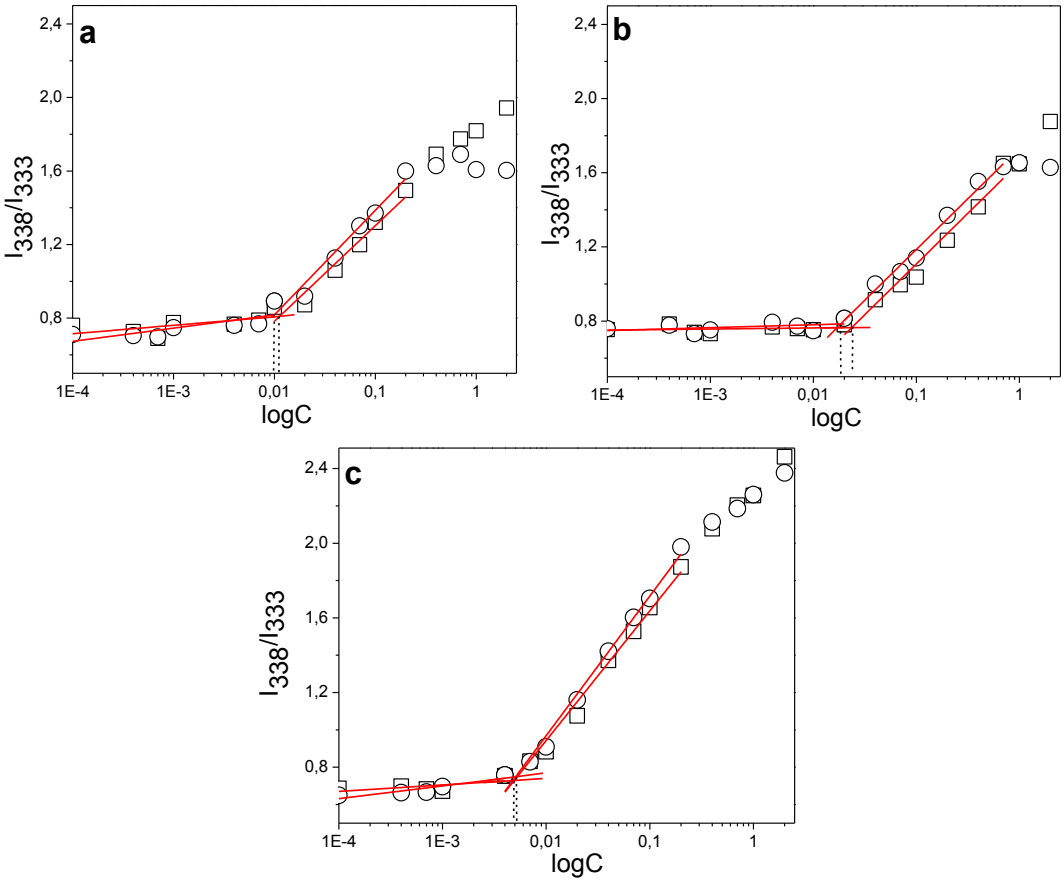

Fig. 4. Dependence of fluorescence intensity ratio (I_{338}/I_{333}) of 6×10^{-7} M pyrene on concentration of copolymer solutions at pH 7 in 0.02 M phosphate buffer. a) □:POEGMA$_{475}$-P4VP1, ○:POEGMA$_{475}$-P4VP2; b) □:POEGMA$_{950}$-P4VP1, ○:POEGMA$_{950}$-P4VP2; c) □:P(DEGMA-*co*-OEGMA$_{475}$)-P4VP1, ○:P(DEGMA-*co*-OEGMA$_{475}$)-P4VP2. Temperature was 15 °C for P(DEGMA-*co*-OEGMA$_{475}$)-P4VP copolymers and 25 °C for POEGMA$_{475}$-P4VP and POEGMA$_{950}$-P4VP copolymers.

rod-like conformation, at pH values below 5.0–5.5. At this pH range, zeta potential values of copolymers are positive and decreases with pH. In addition, copolymers having the same POEGMA block but longer P4VP chains have higher positive charges below pH 5. Taken together, P4VP blocks of copolymers are protonated at acidic pH values and positive charge on copolymers prevents association of unimers to form micelles.

At pH values between 2 and 5, it is important to emphasize that pyrene molecules are entrapped by unimeric polymer structures when Figs. 4–6 are examined together. Below pH 5, I_{338}/I_{333} values were predicted to be identical in Fig. 5 for all copolymers and as low as I_{338}/I_{333} values below *cmc* (Fig. 4) due to the positively charged P4VP blocks. However, it was observed that I_{338}/I_{333} values of all copolymers were constant at higher values in Fig. 5. This indicates the entrapment of pyrene molecules into the copolymer chains. In addition, increase in chain length of POEGMA block and decrease in ethylene glycol number caused an increase in I_{338}/I_{333} value below pH 5. It is clear that copolymers are unimers in solution according to Fig. 6, which reveals that hydrophobic pyrene molecules are entrapped by POEGMA blocks of copolymers, even by most hydrophilic POEGMA block (i.e. POEGMA$_{950}$).

At pH values between 5.0 and 5.5, hydrodynamic diameters of copolymers increase (Fig. 6a) and copolymers become neutral or slightly charged (Fig. 6b). At this pH range, P4VP blocks become neutral and hydrophobic, which allow copolymer unimers to form micelles through hydrophobic interactions. Above pH 5.0–5.5, copolymers with the same POEGMA block but longer P4VP chains (copolymers with P4VP2 blocks) behave differently from the copolymers with shorter P4VP chains (copolymers with P4VP1 blocks). The diameter of copolymers with P4VP2 blocks first increase then reduces with the increase in pH and remains constant at pH values higher than pH 6. This issue may be attributed to the transition of P4VP blocks from hydrophilic to hydrophobic state initiating the formation of micelles. The transition state at which aggregation and micelle formation is not stable (leading to the formation of large aggregates first), is followed by the formation of stable micelles with constant (and smaller) diameters upon increase in pH. This effect is more profound with the copolymers having longer P4VP block (copolymers with P4VP2 blocks). Furthermore, diameters of copolymers with P4VP2 blocks are much smaller than copolymers with P4VP1 blocks at pH values between 6 and 9. Sharp increase and decrease in size is not observed for copolymers with P4VP1 blocks between pH 5 and 6. Size of copolymers with P4VP1 blocks increase to a larger value above pH 5 and then, slight variations are observed in their size upon pH increase. Difference in sizes of copolymers with P4VP2 blocks and copolymers with P4VP1 blocks is only related to length of P4VP block, not to POEGMA block. Longer hydrophobic chains in copolymers with P4VP2 blocks caused to form smaller particles that may be the result of stronger hydrophobic interactions between individual chains and smaller aggregation numbers. These results are also in accord with fluorescence results. In contrast, copolymers with shorter P4VP chains form larger structures as a result of higher aggregation numbers and weaker hydrophobic interactions. Morphology of micelles formed from POEGMA$_{475}$-P4VP1 is shown in AFM image presented in Fig. 7. Spherical particles were observed

Table 2
Critical micelle concentrations (*cmc*) of copolymers obtained from Fig. 4.

Copolymer	*cmc* (mg/mL)
$POEGMA_{950}$-P4VP1	0.025
$POEGMA_{950}$-P4VP2	0.019
$POEGMA_{475}$-P4VP1	0.012
$POEGMA_{475}$-P4VP2	0.010
P(DEGMA-*co*-$OEGMA_{475}$)-P4VP1	0.0051
P(DEGMA-*co*-$OEGMA_{475}$)-P4VP2	0.0048

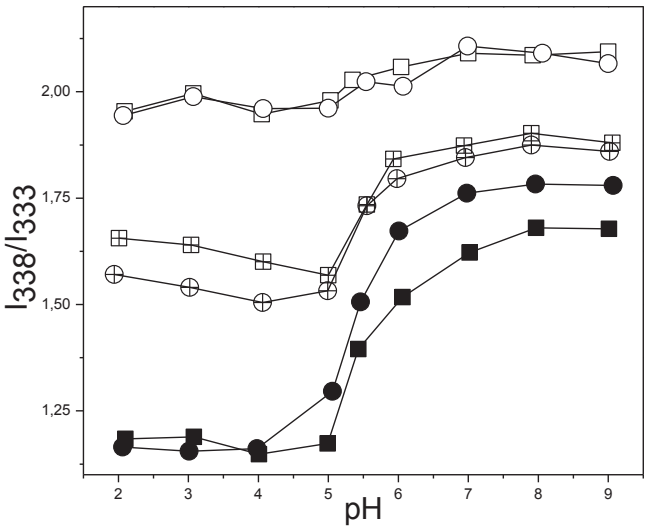

Fig. 5. Dependence of fluorescence intensity ratio (I_{338}/I_{333}) of 6×10^{-7} M pyrene on pH of 1 mg/mL copolymer solutions in 0.02 M phosphate buffer. (⊞:$POEGMA_{475}$-P4VP1; ⊕:$POEGMA_{475}$-P4VP2; ■:$POEGMA_{950}$-P4VP1; ●:$POEGMA_{950}$-P4VP2; □:P(DEGMA-*co*-$OEGMA_{475}$)-P4VP1; ○:P(DEGMA-*co*-$OEGMA_{475}$)-P4VP2). Temperature was 15 °C for P(DEGMA-*co*-$OEGMA_{475}$)-P4VP copolymers and 25 °C for $POEGMA_{475}$-P4VP and $POEGMA_{950}$-P4VP copolymers.

in AFM images and diameter of particles was about 25 nm. When compared with the DLS results, reason of shrinkage in the size of micelles can be the collapse of the core and the shell of micelle particles during the AFM sample preparation process [30].

In Fig. 6b, zeta potential of copolymers is decreasing from positive values to negative values from pH 2 to 9. Number of bonded protons to pyridine rings decrease with pH until pH 5.0–5.5 and pyridine rings become neutral above pH 5.0–5.5. Above pH 5.0–5.5, copolymers form negatively charged micelles. Hydrophilic POEGMA blocks constitute the shell of micelles and α-carboxylic acid end-group of POEGMA blocks remain on the surface of micelles exposing to the aqueous phase. Ionized carboxylic acid groups at shell of micelles make particles negatively charged.

3.4. Effect of temperature on solution behavior of copolymers

Temperature responsive polymers of OEGMA have been synthesized by co-polymerizing DEGMA with OEGMA monomers. LCST value of the final polymer can be tuned by changing the molar ratio of the monomers and number of ethylene glycol units in OEGMA monomer [20]. In our study, we prepared copolymers of DEGMA and OEGMA having 8% mole $OEGMA_{475}$ to obtain thermo-responsive P(DEGMA-*co*-$OEGMA_{475}$) block (LCST 37 °C) [22] and P4VP block was chain-extended from this polymer. Fig. 8a shows transmittance of P(DEGMA-*co*-$OEGMA_{475}$)-P4VP1 and P(DEGMA-*co*-$OEGMA_{475}$)-P4VP2 solutions at pH 3 and 7 as a function of temperature. At pH 7, P4VP blocks in both copolymers are hydrophobic and LCST values of copolymers shifted to lower temperature with increased length of P4VP. Higher hydrophobicity of the structure might have strengthened intramolecular interactions of copolymers between ether groups and amines [31], not with solvent molecules. In contrary, P4VP blocks are positively charged and soluble at pH 3 for both copolymers. In Fig. 8a, LCST values at pH 3 are much higher than the values at pH 7. Increased solubility of P4VP blocks increases interactions with solvent (water) and shifts LCST to higher temperatures. It is important to note that turbidity of copolymer solutions at pH 3 is much lower than the values of copolymer solutions at pH 7. In Fig. 8b, increase in diameters of copolymers is clearly seen at pH 3 and 50 °C. We consider that positively charged POEGMA-*b*-P4VP block copolymers associated together with the effect of hydrophobic POEGMA blocks at the temperatures above LCST. POEGMA blocks formed the core of micelle/aggregates and positively charged P4VP blocks constituted the shell of particles.

4. Conclusion

In the study, we synthesized POEGMA-*b*-P4VP dual responsive amphiphilic block copolymers for the first time. Narrow

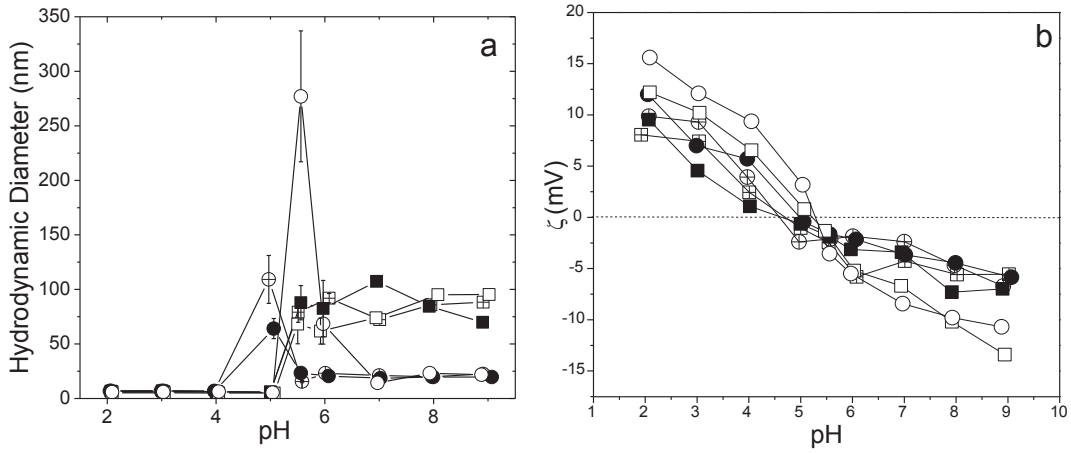

Fig. 6. Hydrodynamic size (a) and zeta potentials (b) of copolymers as a function of solution pH. (⊞:$POEGMA_{475}$-P4VP1; ⊕:$POEGMA_{475}$-P4VP2; ■:$POEGMA_{950}$-P4VP1; ●:$POEGMA_{950}$-P4VP2; □:P(DEGMA-*co*-$OEGMA_{475}$)-P4VP1; ○:P(DEGMA-*co*-$OEGMA_{475}$)-P4VP2). Temperature was 15 °C for P(DEGMA-*co*-$OEGMA_{475}$)-P4VP copolymers and 25 °C for $POEGMA_{475}$-P4VP and $POEGMA_{950}$-P4VP copolymers.

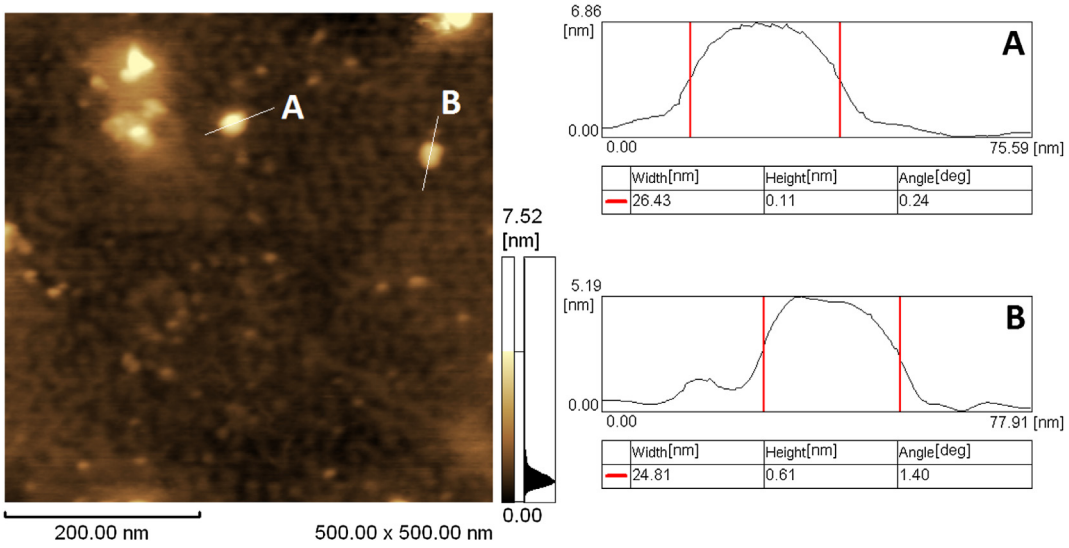

Fig. 7. AFM image and line profiles of POEGMA$_{475}$-P4VP1.

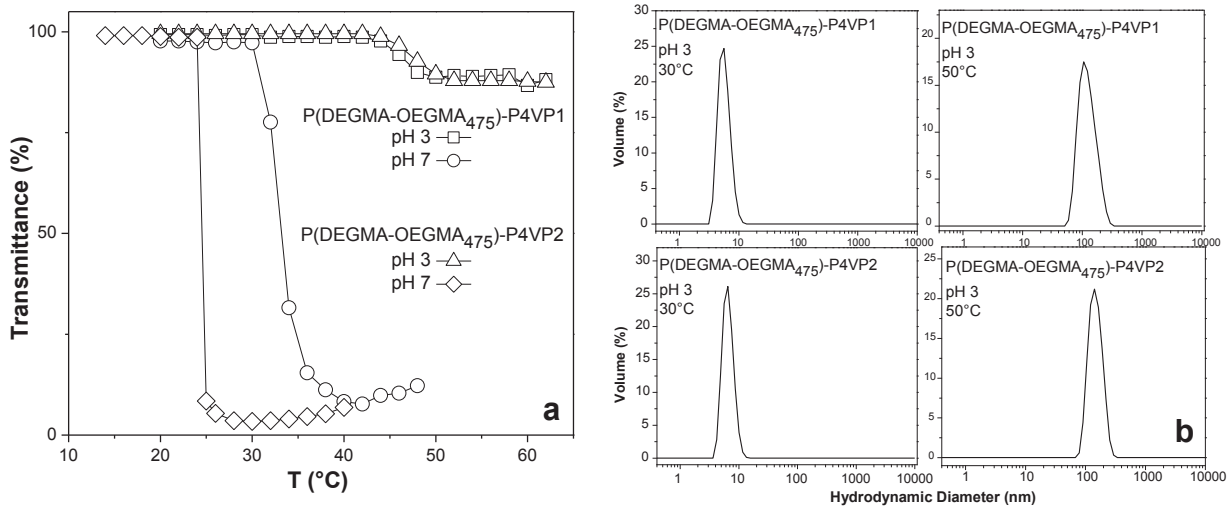

Fig. 8. Turbidity of P(DEGMA-*co*-OEGMA$_{475}$)-P4VP solutions at pH 3 and 7 as a function of temperature (a). Hydrodynamic size distributions of P(DEGMA-*co*-OEGMA$_{475}$)-P4VP copolymers above and below LCST value at pH 3 (b).

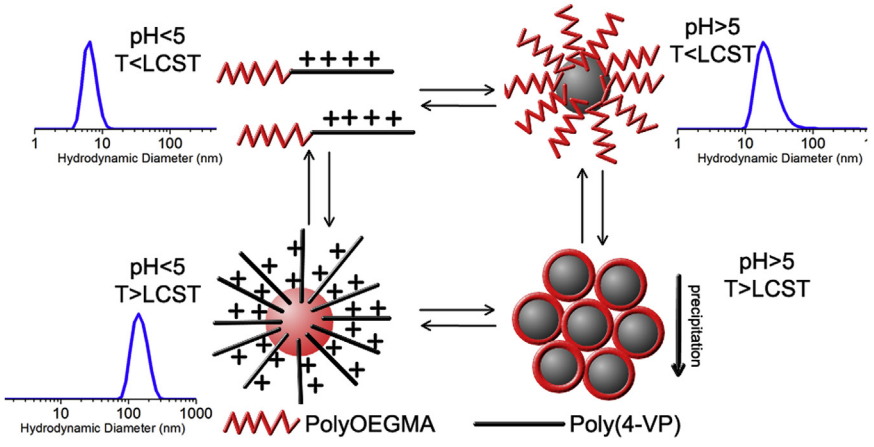

Fig. 9. Schematic representation of formed particles at different pH values and temperatures.

polydisperse copolymers having α-carboxylic acid end-groups were produced using RAFT polymerization technique in two steps. Copolymer chains associated to form micelles at neutral and basic pH values. Size of micelles changed depending on the block ratio of P4VP and POEGMA. Copolymers with a longer P4VP block and the same POEGMA block had smaller hydrodynamic diameters that may be the result of stronger hydrophobic interactions and smaller aggregation numbers. Below pH 5, copolymer unimers were observed owing to the repulsion between positively charged P4VP blocks. However, hydrophobic pyrene molecules were entrapped also by copolymer unimers at acidic pH values by hydrophobic methacrylate chain of POEGMA block. P4VP block significantly altered the LCST value of temperature responsive block copolymers. At neutral pH, LCST value of the copolymers decreased to lower temperatures than the LCST of the macroRAFT agent, P(DEGMA-*co*-OEGMA$_{475}$) polymer. The increase in the length of P4VP block decreased the LCST. At pH 3, LCST of copolymers shifted to higher temperatures due to the increased interaction of copolymers with water through positively charged P4VP block. Fig. 9 summarizes the structures formed at different pH and temperature values and schematically represents the dual-responsive nature of the copolymers.

The copolymers synthesized in this study are versatile building blocks for drug delivery applications. Copolymer structures for specific applications can be produced by tuning easily the molecular weight, composition or number of ethylene glycol units of copolymers. Targeting to specific tissue and localized drug release can be accomplished by internal or external pH and/or temperature stimuli due to the dual responsive nature of the copolymers. In addition, the copolymers allow the conjugation of marker or targeting molecules to the chain end, which would improve the efficiency of the drug carrier system.

Acknowledgments

This study was funded by TUBITAK (The Scientific and Technological Research Council of Turkey) with the project number of 110T570. Authors are grateful to Yasemin Budama Kilinc and Yeliz Basaran Elalmis for their contribution to fluorescence spectrometry and AFM studies, respectively.

References

[1] Kwon GS. Polymeric drug delivery systems. 1 ed. Boca Raton: Taylor & Francis Group; 2005. pp. 535–8.
[2] Smart T, Lomas H, Massignani M, Flores-Merino MV, Perez LR, Battaglia G. Nano Today 2008;3(3–4):38–46.
[3] Allen C, Maysinger D, Eisenberg A. Colloids Surf B Biointerfaces 1999;16(1):3–27.
[4] Jeong Y-I, Nah J-W, Lee H-C, Kim S-H, Cho C-S. Int J Pharmaceut 1999;188(1):49–58.
[5] Cabane E, Zhang X, Langowska K, Palivan CG, Meier W. Biointerphases 2012;7(1–4):1–27.
[6] Hörter D, Dressman J. Adv Drug Deliv Rev 2001;46(1):75–87.
[7] Ganta S, Devalapally H, Shahiwala A, Amiji M. J Control Release 2008;126(3):187–204.
[8] Meyer DE, Shin B, Kong G, Dewhirst M, Chilkoti A. J Control Release 2001;74(1):213–24.
[9] Ali M, Brocchini S. Adv Drug Deliv Rev 2006;58(15):1671–87.
[10] Boyer C, Bulmus V, Davis TP, Ladmiral V, Liu J, Perrier S b. Chem Rev 2009;109(11):5402–36.
[11] Chiefari J, Chong Y, Ercole F, Krstina J, Jeffery J, Le TP, et al. Macromolecules 1998;31(16):5559–62.
[12] McCormick CL, Lowe AB. Acc Chem Res 2004;37(5):312–25.
[13] York AW, Kirkland SE, McCormick CL. Adv Drug Deliv Rev 2008;60(9):1018–36.
[14] Borchert U, Lipprandt U, Bilang M, Kimpfler A, Rank A, Peschka-Süss R, et al. Langmuir 2006;22(13):5843–7.
[15] Liu F, Eisenberg A. J Am Chem Soc 2003;125(49):15059–64.
[16] San Juan A, Letourneur D, Izumrudov VA. Bioconjug Chem 2007;18(3):922–8.
[17] Allison BC, Applegate BM, Youngblood JP. Biomacromolecules 2007;8(10):2995–9.
[18] Stratton TR, Rickus JL, Youngblood JP. Biomacromolecules 2009;10(9):2550–5.
[19] Badi N, Lutz J-F. J Control Release 2009;140(3):224–9.
[20] Lutz JF. J Polym Sci Part A Polym Chem 2008;46(11):3459–70.
[21] Becer CR, Hahn S, Fijten MW, Thijs HM, Hoogenboom R, Schubert US. J Polym Sci Part A Polym Chem 2008;46(21):7138–47.
[22] Lutz J-F, Hoth A. Macromolecules 2006;39(2):893–6.
[23] Hu YQ, Kim MS, Kim BS, Lee DS. Polymer 2007;48(12):3437–43.
[24] Rossi NA, Jadhav V, Lai BF, Maiti S, Kizhakkedathu JN. J Polym Sci Part A Polym Chem 2008;46(12):4021–9.
[25] Zeng J, Shi K, Zhang Y, Sun X, Deng L, Guo X, et al. J Colloid Interface Sci 2008;322(2):654–9.
[26] Wilhelm M, Zhao CL, Wang Y, Xu R, Winnik MA, Mura JL, et al. Macromolecules 1991;24(5):1033–40.
[27] Pietsch C, Fijten MW, Lambermont-Thijs HM, Hoogenboom R, Schubert US. J Polym Sci Part A Polym Chem 2009;47(11):2811–20.
[28] Barner-Kowollik C, Buback M, Charleux B, Coote ML, Drache M, Fukuda T, et al. J Polym Sci Part A Polym Chem 2006;44(20):5809–31.
[29] Torchilin VP. Pharm Res 2007;24(1):1–16.
[30] Xiong D a, He Z, An Y, Li Z, Wang H, Chen X, et al. Polymer 2008;49(10):2548–52.
[31] Jones JA, Novo N, Flagler K, Pagnucco CD, Carew S, Cheong C, et al. J Polym Sci Part A Polym Chem 2005;43(23):6095–104.